Positron induced electron emission from graphene

IOP Conf. Series: Journal of Physics: Conf. Series **791** (2017) 012033 doi:10.1088/1742-6596/791/1/012033

Positron induced electron emission from graphene

V A Chirayath[1], R W Gladen[1], K Shastry[1], M D Chrysler[1], A J Fairchild[1], A D McDonald[1], A R Koymen[1], B Barbiellini[2] and A H Weiss[1]

[1]Dept. of Physics, University of Texas at Arlington, Arlington 76019-0059, USA
[2]Dept. of Physics, Northeastern University, Boston, MA 02115, USA

email: chirayat@uta.edu

Abstract. We report here the energy spectra of positron-induced electrons emitted from single- and multilayer graphene films. One of UT Arlington's two Time of Flight positron beam systems was used to deposit very low energy (KE < 1.5 eV) positrons at the surface of graphene samples consisting of a) 1 layer of graphene on polycrystalline Cu and b) 6-8 layers of graphene deposited on polycrystalline Cu. A time of flight spectrometer was used to measure the energy of positron-induced electrons. A peak in the electron energy spectrum was observed at ~263 eV corresponding to annihilation induced Auger electrons as a result of the KVV transition from the two graphene samples, which were comparable in intensity to that observed from a bulk graphite sample. In addition, we have observed a low energy peak in the annihilation induced electron energy spectra from graphene which extends up to ~15 eV. Our observation that the positron annihilation induced KVV Auger signal from graphene has a significant intensity indicates that the low energy positrons can be efficiently trapped on the surface of graphene layer on Cu down to a single-layer.

1. Introduction

Low energy positrons incident on a surface induce electron emission through several mechanisms. Secondary electron emission resulting from positron impact was observed in the first measurements with a low energy positron beam [1-3]. Weiss *et al.* [4] identified a second process in which electron emission occurred as a result of an Auger transition involving the filling of core hole created by electron-positron annihilation. This effect resulted in a new surface characterization technique called positron annihilation induced Auger electron spectroscopy (PAES). Since the starting core hole is created through an annihilation process, a PAES signal can be obtained with arbitrarily low positron beam energies. The secondary and redistributed primary background, which makes quantitative analysis difficult in electron induced Auger electron spectroscopy (EAES), can be completely eliminated as a result of this merit. Moreover, PAES has superior surface sensitivity due to the fact that almost all of the signal stems from the annihilation of positrons trapped in a surface state localized at an image potential well just outside the topmost layer of surface atoms [5]. Recently Mukherjee *et al.* [6] identified a third process by which positrons can induce electron emission. They observed a secondary electron peak for positron beam energies well below the electron work function. In this process, the energy released during the transition of a positron from a positive energy scattering state directly into a bound surface state is taken up by an electron near the Fermi level, giving it enough

energy to escape. Because of the similarity with an Auger transition, this process was named Auger mediated positron sticking (AMPS).

Application of conservation of energy shows that the AMPS process can lead to electron emission when the incident positron beam energy is above a threshold: $E_{th,AMPS} = \phi^- - E_{SS}$, where ϕ^- is the electron work function, E_{SS} is the positron surface state binding energy and $E_{th,AMPS}$ is the threshold for the AMPS process. Mukherjee *et al.* [6] used this relation and an experimental determination of the AMPS threshold energy to obtain an independent estimate of the binding energy of the positrons in the surface state of copper and gold which was in close agreement with previous estimates based on positronium thermal desorption measurements. A similar argument shows that the threshold energy, $E_{th,sec}$, for electron emission in the case where the positron first makes a transition to a bulk state can be written as $E_{th,sec} = \phi^- - \phi^+$ where ϕ^+ is the positron work function (binding energy of positrons in the bulk ground state) and $E_{th,sec}$ is the threshold for secondary electron emission. Typically $E_{SS} > \phi^+$ and consequently $E_{th,AMPS} < E_{th,sec}$. AMPS is the only significant non-annihilation induced electron emission process for positrons incident in the energy range above $E_{th,AMPS}$ and below $E_{th,sec}$. Once the incident positron energy is greater than $E_{th,sec}$ by a few eV, non-annihilation induced electron emission is dominated by processes in which the positron loses energy to an electron while making a transition into a bulk state.

It should be noted that the yield of secondary electrons due to the photo-absorption or Compton scattering of annihilation gamma rays is estimated to be smaller than 10^{-6} electrons per incident positron by taking the ratio of the secondary electron escape depth to the gamma adsorption length. This estimate is consistent with the experimental observation that the gamma induced electron background is negligible compared to yield of electrons resulting from secondary emission, annihilation induced Auger emission or the AMPS process.

In this paper, we report the energy spectra of electrons emitted from single and multilayer (6-8 layers) graphene on a polycrystalline Cu substrate at different positron kinetic energies. The spectra, taken with an incident positron kinetic energy of 1.5 eV, allowed us to observe a new low energy electron emission peak from single and multilayer graphene layers deposited on Cu, which is not present on the clean Cu surface. It is posited that this emission feature is associated with Auger like processes initiated by the creation by positron annihilation of a deep hole in the valence band.

2. Experimental apparatus and sample

The experimental apparatus, consisting of a low energy positron beam equipped with a time of flight spectrometer, has been described in detail in a previous publication [7]. However, for completeness, the key features of the system are described here. Slow positrons are obtained using a 10 mCi Na^{22} source mount with a tungsten moderator in transmission geometry. The slow positrons are filtered from the fast positrons using mutually perpendicular magnetic and electric fields generated using a set of electrically biased plates (**E×B** plates**)** and an axial magnetic field (~ 100 Gauss). This is followed by a nine stage graded accelerator /decelerator which enables us to accelerate or decelerate the positrons by appropriate biasing.

The time of flight (TOF) spectrometer and sample were biased so as to allow us to measure the energy of electrons emitted from the sample with kinetic energies from 0 eV to 500 eV. The micro-channel plate (MCP) detector used for the detection of electrons emitted from the sample is in the path of the positron beam. An additional set of **E×B** plates (C and D in figure 1) is used to bend the positrons around the MCP. The positrons then fly through a grounded TOF tube (~ 600 cm) before reaching the sample. The magnetic field at the TOF region and the MCP is kept at 40 Gauss. A permanent magnet kept behind the sample produces a large magnetic field gradient near the sample. The field on the surface of the sample because of this permanent magnet is ~450 Gauss. The magnetic field gradient from the sample to the entrance of TOF tube reduces the transverse velocity component of the emitted electrons as a result of positron implantation and thus reduces the width of the distribution of TOF of electrons emitted from the sample [7, 8]. The electrons, after entering the TOF tube, travel through a field free region and are deflected by the **E×B** plates, D, onto the MCP.

The two 511 keV gammas produced after positron annihilation with electrons from the sample are detected by a BaF_2 scintillation detector and a NaI(Tl) detector placed on opposite sides of the sample. The TOF of the electrons are determined by the time difference between the signal generated by the BaF_2 scintillation detector after the detection of 511keV gamma and the signal generated by the MCP after electron detection. The experiment was performed using "reverse timing" in which the gamma signal was delayed and used as the stop signal to the time to amplitude converter (TAC). The MCP signal is used as the start signal. A histogram of the time of flight is generated from the TAC output using a multichannel analyzer. The TOF histogram is converted to an energy histogram by using an appropriate conversion function determined experimentally using the secondary electron peak generated at different incident positron energies. The relation between TOF and the inverse of the square root of energy is expected to be linear, though higher order corrections are required to correct for the time electrons spend between the **E×B** plates.

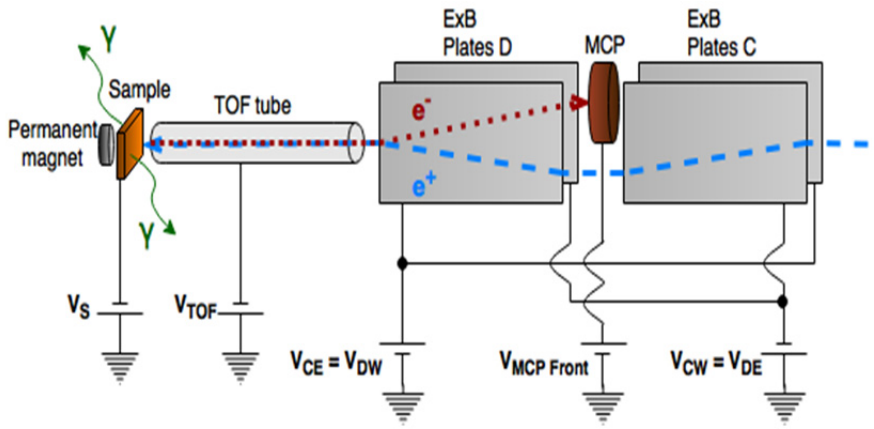

Figure 1. Shows the schematic of the TOF spectrometer attached to the positron beam system. **E×B** plates C and D bends the positrons (blue dash) around the MCP. The electrons (red dots) emitted from the sample after annihilation of positrons are bend by **E×B** plates D into the MCP. The TOF tube is connected to ground for the present experiment and the sample is applied a negative potential with respect to the TOF tube.

2.1. Sample

Single-layer graphene and 6-8 layers graphene grown on polycrystalline Cu using chemical vapor deposition was purchased from ACS materials. The samples were characterized with Raman spectroscopy and the presence of single-layer and multi-layer graphene were confirmed from the shape of the 2D band at ~ 2700 cm^{-1} [9]. The analysis chamber was kept at a vacuum of 1.33×10^{-8} Pa during measurements. The single-layer graphene on polycrystalline Cu was sputter cleaned in Argon atmosphere at a vacuum of 8×10^{-3} Pa and at a sputter current of <1 μA to obtain a clean sample of polycrystalline Cu. It was observed that the Auger peak of Cu could be obtained within minutes of sputtering which is indicative of the presence of clean Cu on which graphene was grown. The data on polycrystalline Cu shown here were collected after Auger peaks of carbon or oxygen were completely absent after sputtering out the single-layer graphene over-layer. In order to avoid contamination by surface adsorption, the polycrystalline Cu was sputtered every 14 hours during data acquisition.

3. TOF-PAES results

In order to obtain the Auger spectrum free from secondary electron background, it was important to set the incident kinetic energy of the positron at the sample below the threshold required for secondary electron emission in Cu and graphene. This threshold was found to be ~2 eV [7]. We have achieved beam settings that allow both positron and electron transport at these very low energies. For these

settings, measurements of the positron kinetic energy showed that almost all positrons had a kinetic energy less than 1 eV [10] while traveling through the grounded TOF tube. The kinetic energy of positrons hitting the sample surface was determined by adding a term:

$$\Delta KE = e(-V_s) + (\phi^-_s - \phi^-_{TOF\ tube}), \quad (1)$$

to the kinetic energy of the positrons measured at the TOF tube. Here e, V_s, ϕ^-_s, and $\phi^-_{TOF\ tube}$ are the charge of the electron, the sample bias, the electron work functions of the sample and TOF tube respectively. $(\phi^-_s - \phi^-_{TOF\ tube})$ takes into account the contact potential developed between the sample and the TOF tube because of the difference in their electron work functions. For the settings used in this work, the maximum KE of positrons hitting the sample, KE_s, was taken to be equal to ΔKE +1 eV.

3.1. Electron Energy Spectra Obtained with Positron Incident below the AMPS Threshold

The TOF-PAES spectra obtained with a positron kinetic energy of 1.5 eV are shown in figure 2. The spectra of polycrystalline Cu, single-layer graphene and multilayer graphene are shown together for comparison of various spectral features. The TOF's are sampled at an interval of ~0.00195 μs from 0 to 4μs. The peaks are identified after converting the TOF to energy using the non linear conversion function and have been labeled in the figure. The energy per TOF increases as TOF decreases which causes the low energy peaks to be broader and the high energy Auger peaks to be sharper in the TOF spectrum. At a TOF of 1.3 μs which corresponds to 15 eV, energy increases by 0.15 eV per TOF step where as at a TOF of 1 μs which corresponds to 350 eV, energy increases by 16 eV per TOF step. All data are normalized to the counts under the 511 keV peak as detected by NaI (Tl) detector. The PAES spectrum from Cu shows the $M_{2,3}VV$ peak and M_1VV peak at 60 eV and 108 eV respectively. Spectral intensity for TOF flights above 1.2 μs in the electron spectra from Cu is mostly due to the inelastic loss of the Auger peaks. Within the detection limit of the experiment neither carbon nor oxygen are present on the surface of polycrystalline Cu. The spectral weight under the inelastic tail (defined up to ~15 eV) is approximately three times the intensity in $M_{2,3}VV$ peak at 60 eV.

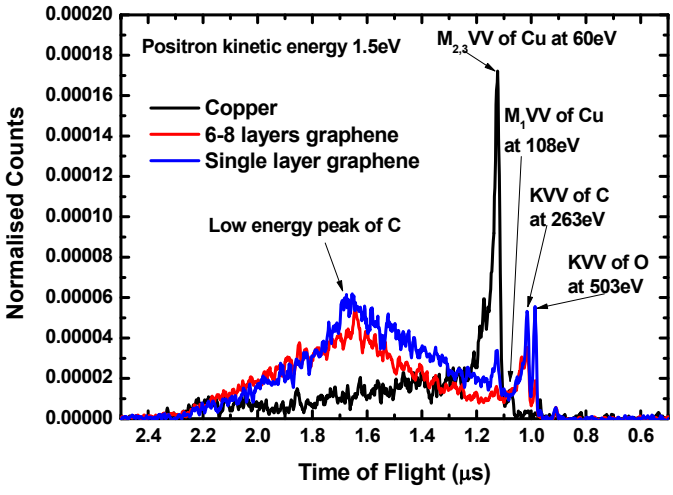

Figure 2. TOF spectra of electrons resulting from positrons incident at 1.5 eV on single and multilayer graphene (deposited on Cu) and clean Cu. The sample was biased at -0.5 V in each case. Major peaks, corresponding to Auger transitions in Cu and C, are labeled along with their corresponding energies. The counts in the TOF spectra have been normalized to annihilation gamma counts. (color online)

The spectra of single-layer and multilayer graphene show Auger peaks corresponding to KVV transition in Carbon at 263 eV. It was found that the intensity of KVV peak is comparable to that obtained from graphite [10]. Therefore, low energy positrons can be trapped efficiently on the surface state of graphene down to a single-layer of graphene. Both single-layer graphene and multilayer graphene show presence of adsorbed oxygen on the surface through the Auger peak corresponding to KVV transition in oxygen. However, the intensity of oxygen peak is higher in single-layer graphene than in multilayer graphene, which is indicative of the surface chemical reactivity of single-layer

graphene compared to multilayer graphene. The data from single-layer graphene shows a peak corresponding to the $M_{2,3}VV$ Auger transition in Cu which has ~ 0.2 times the intensity under the $M_{2,3}VV$ peak observed for the clean Cu surface. This indicates that there is significant overlap of the positron surface state wave function with Cu atoms even though the graphene film is expected to be continuous. A possible explanation for this overlap is that the positron surface state on single-layer graphene has significant penetration into the interface between the graphene layer and Cu substrate [9]. In contrast, it may be seen in figure 2 that the Cu $M_{2,3}VV$ peak is barely visible in the spectra obtained from multilayer graphene on Cu.

A key feature in the Auger spectra of graphene (both single-layer and multilayer) is a broad peak at ~1.75 μs. Note that this peak is not seen in the spectra of clean Cu. The higher intensity in the broad peak for single-layer graphene when compared to multilayer graphene could be due to the additional contributions of the inelastic tail of the $M_{2,3}VV$ peak of Cu present in the single-layer graphene spectra. The broad peak cannot be accounted for in terms of the inelastic tail of the KVV peaks of carbon or oxygen as its shape, and more importantly, its intensity (~ 16 times the KVV peak at 263 eV) does not follow the expected trend of an Auger inelastic tail (of which the tail seen in the Cu spectra is typical). A similar broad peak was also seen for highly oriented pyrolytic graphite [10]. Since the incident positron energy was below both secondary electron and AMPS threshold, energy considerations rule out non-annihilation induced processes for the production of the peak between 2 μs to 1.3 μs (corresponding to an energy range of 2 eV to 15 eV). Considering that the intensity of the low energy peak is more than 6 times larger than the C KVV PAES peak (which is associated with the annihilation of C 1s electrons) we posit that the low energy peak is due to the annihilation of the positrons with valence electrons. It is energetically possible to account for the observed upper bound of ~15 eV on the low energy peak in terms of known width and depth of the valence band of graphene [11]. A hole created deep enough in the valence band can result in an intra-band Auger process releasing enough energy for a third electron from the band to make transition to states outside vacuum. Such transitions are extremely difficult to observe in photoemission spectroscopy or in conventional electron Auger spectroscopy because of the background of photoelectrons or secondary electrons [12]. To our knowledge ours is the first direct observation of this low energy spectral feature in graphene.

3.2. Electron Energy Spectra Obtained with Positron Incident above the AMPS and Secondary emission threshold

Panels (a)-(d) in figure 3 show a series of TOF positron induced electron spectra taken with increasingly more negative sample biases. An increase in the magnitude of the (negative) sample bias results in an increase of ΔKE (see eq. 1) in the kinetic energy of positrons hitting the surface. The negative bias also results in a corresponding acceleration and increase in the energies of electrons as they travel from the sample and enter into the TOF tube. This increase results in a shift of the entire TOF spectrum to the right (lower TOF), as the lowest energy of the electrons starting from the sample varies from 0 eV to a value equal to ΔKE. Referring to figure 3, as the incident positron kinetic energy increases above the AMPS threshold, a low energy peak becomes visible in both Cu and graphene TOF spectra as shown in figure 3 (a) and (b). In graphene, the AMPS feature is merged with the low energy peak and hence it appears as a shoulder on the low energy peak. The presence of an AMPS peak at the incident positron energy of 2 eV and 2.5 eV demonstrates the efficient trapping of positrons on the surface state of a single-layer graphene. When the positron energy reaches a value above the threshold for secondary emission, the spectra at low electron energies are dominated by secondary electrons emitted from the bulk. By the time the positron kinetic energy reaches 6 eV, the spectral contributions of positron induced secondary electron emission merge with the low energy C peak seen in panel (a) and they mask it. The difficulty of separating the low energy C peak from a secondary background helps explain the failure of conventional surface spectroscopic methods in detecting this peak previously. Note that the distribution of the positron impact induced secondary electrons from Cu is different from that obtained from a single-layer graphene on Cu (see figure 3 (c) and (d)). Changes observed in the electron induced secondary electron spectrum at low energies

caused by the adsorption of graphene on a metal have been ascribed to changes in the surface density of states [13]. The large changes seen in our data in going from clean Cu to single layer graphene indicate that positron induced secondary electron spectra are even more sensitive to changes in the surface density of states.

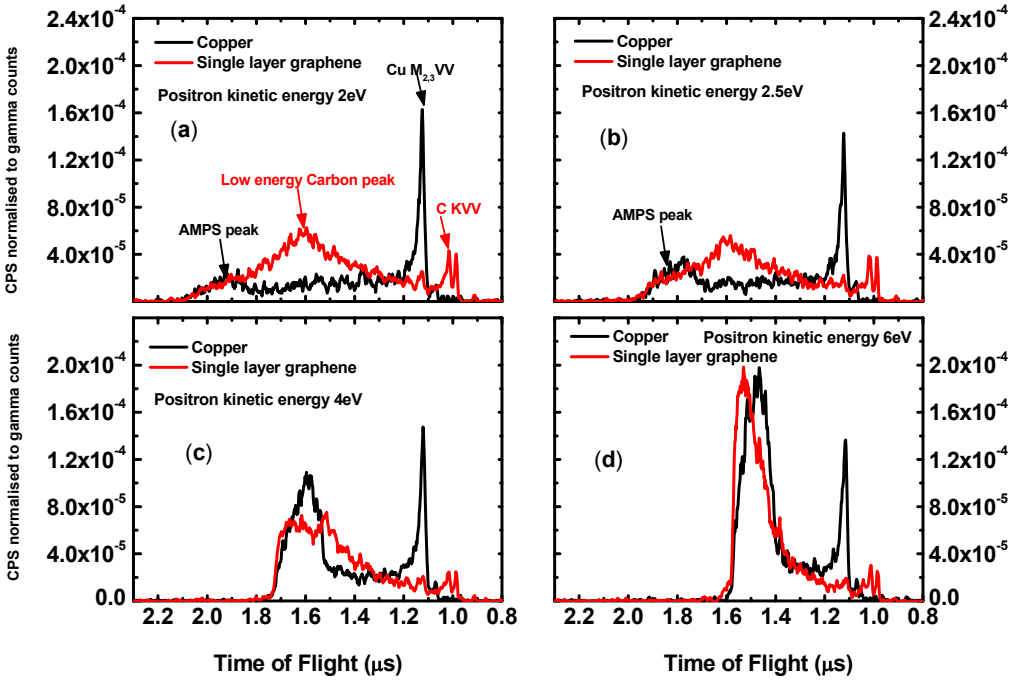

Figure 3. TOF spectra of positron induced electrons emitted from a single-layer of graphene on Cu and from clean Cu taken for sample biases: (a) -1.5V (b) -2.V (c) -3.5 V and (d) -5.5V (corresponding to incident energies of 2 eV, 2.5 eV,4 eV, and 6 eV respectively). Note: an increase in the magnitude of the (neg.) sample bias results in an increase in the kinetic energy (and a decrease in the time of flight) of electrons emitted from the sample as they traverse the TOF analyzer.(color online)

4. Conclusion

A very low energy positron beam was used to obtain the spectrum of positron annihilation induced electrons from surfaces consisting of a single and multilayer graphene on polycrystalline Cu and clean polycrystalline Cu. The backgrounds from non-annihilation related electron emission processes were eliminated by maintaining the incident positron kinetic energy below the threshold for electron emission through either impact induced secondary emission or the AMPS process. A strong positron annihilation induced Auger peak corresponding to KVV transition in carbon was observed for both single-layer and multilayer graphene indicating that positrons are trapped efficiently in surface state on top of graphene. The very low background obtained with 1.5 eV incident positron beam allowed us to observe a low energy feature in the Auger spectra of graphene that is ~ 16 times the intensity in the carbon KVV peak. We posit that these emitted electrons are a result of the filling of deep holes in the graphene valence band that were created by the annihilation of positrons in a bound surfaces state.

Acknowledgment

This work was supported by NSF grant DMR 1508719.

References

[1] Cherry W H 1958 PhD Thesis Princeton University
[2] Mayer R and Weiss A 1988 *Phys.Rev. B* **38** 11927; Mayer R, Gramsch E and Weiss A 1989 *Phys. Rev. B* **40** 11287
[3] Overton N and Coleman P G 1997 *Phys. Rev. Lett.* **79** 305
[4] Weiss A, Mayer R, Jibaly M, Lei C, Mehl D and Lynn K G 1988 *Phys. Rev. Lett.* **61** 2245
[5] Fazleev N G, Fry J L and Weiss A H 2004 *Phys. Rev. B.* **57** 12506
[6] Mukherjee S, Nadesalingam M P, Guagliardo P, Segeant A D, Barbiellini B, Williams J F, Fazleev N G and Weiss A H 2010 *Phys. Rev. Lett.* **104** 247403
[7] Mukherjee S, Shastrty K, Anto C V, Joglekar P V, Nadesalingam M P, Xie S, Jiang N and Weiss A H 2016 *Rev. Sci. Instrum.* **87** 035114
[8] Fairchild A J, Chirayath V A, Gladen R W, Chrysler M D, Koymen A R and Weiss A H 2017 *Journal of Physics. Conference Series*. in this volume
[9] Chirayath V A, Chrysler M D, Mcdonald A D, Gladen R W, Fairchild A J, Koymen A R and Weiss A H 2017 *Journal of Physics. Conference Series*. in this volume
[10] Gladen R W, Chirayath V A, Chrysler M D, Mcdonald A D, Fairchild A J, Shastry K, Koymen A R and Weiss A H 2017 in this volume
[11] Ooi N, Rairkar A and Adams J B 2006 *Carbon* **44** 231
[12] Braicovich L 1981 Comparing Valence Auger Lineshapes and Photoemission Spectra: The Cd and CdO Cases *Emission and Scattering Techniques - Studies of Inorganic Molecules, Solids, and Surfaces* (Nato Science Series C, vol 73) ed P Day (Netherlands: Springer) chapter 15 pp 375-384
[13] Riccardi P, Cupolillo A, Pisarra M, Sindona A and Caputi L S 2010 A*ppl. Phys. Lett.* **97** 221909; Riccardi P, Cupolillo A, Pisarra M, Sindona A and Caputi L S 2012 A*ppl. Phys. Lett.* **101** 183102